Morphological instability of crystal growth in nonsteady potentiostatic electrodeposition. I. The mechanism of growth of random crystals in metal deposition

Ryoichi Aogaki and Tohru Makino

Citation: The Journal of Chemical Physics **81**, 2154 (1984); doi: 10.1063/1.447840
View online: http://dx.doi.org/10.1063/1.447840
View Table of Contents: http://scitation.aip.org/content/aip/journal/jcp/81/4?ver=pdfcov
Published by the AIP Publishing

Morphological instability of crystal growth in nonsteady potentiostatic electrodeposition. I. The mechanism of growth of random crystals in metal deposition

Ryoichi Aogaki and Tohru Makino[a)]
Department of Chemistry, The Institute of Vocational Training, 1960, Aihara, Sagamihara, 229, Japan

(Received 19 November 1982; accepted 6 March 1984)

The growth mechanism of irregular, roundish crystals, which commonly appear in potentiostatic deposition, was studied from the viewpoint of the growth of surface fluctuations which originate at an electrode surface. As a result, it was suggested that such irregular crystals come from the initial surface fluctuations caused by the microscopic dissolution and deposition of the electrode surface in thermodynamical equilibrium. After deriving the relationship between the spatial wave number of the fluctuation and the degree of surface irregularity (dsi), the fluctuation component with a single wave number was examined. As for actual fluctuations, since numerous components with different wave numbers are superimposed, it was necessary for graphic simulations by use of computers to be performed. However, from the analysis of only a single wave component, it was concluded that, at high cathodic overpotential, surface diffusion of adatoms exhibits a remarkable effect, viz., if there is no surface diffusion, it can be predicted that very small crystal peaks are rapidly formed owing to multiple nucleation based on the high supersaturation of adatoms; this prediction, however, is not consistent with actual observations. According to the theoretical equation obtained in the present paper, it was clearly concluded that crystal growth at high cathodic polarizations is moderated by the surface diffusion of adatoms, which are released from the concentrated nucleation sites to active lattice points, such as kinks and steps. Moreover, it was also found that the surface energy of the electrode should become constant in value at high cathodic potentials.

I. INTRODUCTION

In a diffusion-limited electrodeposition, a large number of roundish, minute peaks without any particular crystal faces, often emerge on electrode surface.[1-3] The kinetics of such crystal growth, as mentioned before,[4] can be explained obviously from the instability accompanying bulk diffusion of active metal ions. All the analyses which have been established in the preceding papers, are based on whether or not the surface fluctuations arising from microscopic dissolution and deposition at an electrode surface, develop with increasing deposition time. Using this idea, the theory was gradually extended to some cases of deposition.[5,6] Then, in order to compare various theoretical predictions with actual observations, a general expression representing how the initial fluctuations develop into macroscopic, three-dimensional surface irregularities was derived.[6]

First, the expression was applied to a galvanostatic case of electrodeposition.[7,14,15] Three-dimensional contour plots of the electrodeposited surface were drawn by means of computer graphics. Theoretical and statistical data, viz., the average crystal size and its standard deviation, were calculated. Finally, it was concluded that the crystal peak sizes and shapes predicted by the theory were in good agreement with SEM observations.

In the present paper, potentiostatic deposition, another typical condition for electrodeposition was discussed in terms of the theoretical equations. For potentiostatic deposition, the steady state case has already been theoretically treated.[4] Using the equations obtained, the sudden appearance of powdery, minute crystals at high cathodic potentials could be interpreted. However, the theory also predicted a quite large dependence for both the crystal particle dimensions and the growth rate on electrode potential at high cathodic polarizations, i.e., the crystal sizes drastically decrease, ultimately converging to zero while their growth rates increase toward infinity as cathodic potentials are increased. These are severe discrepancies because, according to experiments, the average crystal size and growth rate do not depend on the potential in the high cathodic region but remain almost constant. By introducing surface diffusion effects involving metal adatoms in order to solve the difficulties, we have attempted to establish an instability theory for nonsteady potentiostatic electrodeposition.[8]

II. THEORETICAL

A. Mass transfer of active ionic species

After applying a given potential step to a flat working electrode at a time $t = 0$, active metal ionic species in the neighborhood of the interface continuously deposit on the electrode. Subsequently, in the presence of high concentration of supporting electrolyte, nonsteady transfer of the ion takes place according to the following equation:

$$\frac{\partial C(x,y,z,t)}{\partial t} = D\nabla^2 C(x,y,z,t), \tag{1}$$

where $C(x,y,z,t)$ is the concentration of depositing ion, D is the diffusion coefficient, and $\nabla \equiv (\partial/\partial x, \partial/\partial y, \partial/\partial z)$.

[a)] Present Address: AHS Japan Co., 2-10-12, Akasaka, Minato-ku, 107, Japan.

 0021-9606/84/162154-10$02.10

The electrode reaction is accompanied with a diffusion layer extending into the bulk of the solution. Taking the electrode surface parallel to the x–y plane, it seems reasonable, if there is no fluctuation, to assume that the concentration has a distribution only in the z direction vertical to the surface. In this case, Eq. (1) can be written as

$$\frac{\partial C^*(z,t)}{\partial t} = D\frac{\partial^2 C^*(z,t)}{\partial z^2}. \tag{2}$$

Boundary and initial conditions are

$$t = 0;\ C^*(z,t) = C^*(z=\infty), \tag{3}$$

$$t \neq 0;\ C^*(Z^*,t) = C^*(z=Z^*). \tag{4}$$

Here, $z = Z^*$ denotes the average surface height, and $C^*(z=\infty)$ and $C^*(z=Z^*)$ are the bulk and surface concentrations. From Eqs. (2)–(4), the well-known equation for nondisturbed current density $J_z^*(t)$ is derived,

$$J_z^*(t) = -nF\sqrt{\frac{D}{\pi t}}\{C^*(z=\infty) - C^*(z=Z^*)\}, \tag{5}$$

where $J_z^*(t)$ is defined negative for cathodic current.

On the other hand, perturbing components, originating from the fluctuation of microscopic dissolution and deposition at the electrode, are always imposed on the nondisturbed component. If the perturbations are small, we can write the concentration as $C(x,y,z,t) = C^*(z,t) + c(x,y,z,t)$, where $c(x,y,z,t)$ is the perturbing component of the concentration. Therefore, from Eq. (1), the following equation involving $c(x,y,z,t)$ is obtained:

$$\frac{\partial c(x,y,z,t)}{\partial t} = D\nabla^2 c(x,y,z,t). \tag{6}$$

In general, arbitrary, small fluctuations can be expressed in the form of integration of Fourier components, i.e., in the present case, two-dimensional x–y plane waves

$$c(x,y,z,t) = \frac{1}{2\pi}\int_{-\infty}^{\infty}\int_{-\infty}^{\infty} c^0(z,t) \times \exp[i(k_x x + k_y y)]\, dk_x\, dk_y, \tag{7}$$

where k_x and k_y are the $x-$ and $y-$ components of wave number k, and $c^0(z,t)$ is a Fourier image function of $c(x,y,z,t)$ concerning coordinates x and y, i.e.,

$$c^0(z,t) = \frac{1}{2\pi}\int_{-\infty}^{\infty}\int_{-\infty}^{\infty} c(x,y,z,t) \times \exp[-i(k_x x + k_y y)]\, dx\, dy. \tag{8}$$

Performing Fourier transformation of both sides of Eq. (6) with regard to x and y, the following equation is obtained:

$$\left(\frac{1}{D}\frac{\partial}{\partial t} - \frac{\partial^2}{\partial z^2} + k^2\right)c^0(z,t) = 0, \tag{9}$$

where $k \equiv (k_x^2 + k_y^2)^{1/2}$. This equation can be solved under quasisteady conditions, where the time variation of $c^0(z,t)$ is much smaller than its spatial variation, i.e.,

$$\left|\frac{\partial c^0(z,t)}{\partial t}\right| \ll |Dk^2 c^0(z,t)|.$$

Namely, the general solution for Eq. (9) is

$$c^0(z,t) = (A_1 e^{-kz} + A_2 e^{kz})\alpha(t), \tag{10}$$

where A_1 and A_2 are arbitrary constants, and $\alpha(t)$ is an arbitrary function of t. In the bulk of the solution, $c^0(z,t)$ for $z\to\infty$ should not diverge to infinity, so that $A_2 = 0$ is derived. Therefore, Eq. (10) is rewritten in the form

$$c^0(z,t) = A_1 e^{-kz}\alpha(t). \tag{11}$$

B. Thermodynamic condition accompanied with the mass transport in the electrolyte solution

The electrochemical potential of active species in the solution also changes during the progress of the electrode reaction and, consequently, the species diffuse in the bulk solution. As is well known, this is a dissipative process in thermodynamics. Thus, it can be reasonably assumed that the value of the potential can be uniquely determined at any point in the solution, i.e., the solute particles become transferred, keeping local equilibrium (11).

If the potential is denoted as $\Psi(x,y,z,t)$, such assumption gives the condition that the variation $\delta\Psi(x,y,z,t)$ remains equal to zero, i.e.,

$$\delta\Psi(x,y,z,t) = 0. \tag{12}$$

This is the necessary condition for the minimum of $\Psi(x,y,z,t)$. If we measure the electrode potential by use of an electrode reversible to the active species, taking the potential in the bulk of the solution as a reference, we can determine the electrode potential from the electrochemical potential in the solution. Thus, the equation

$$\Psi(x,y,z,t) = nFV(x,y,z,t) \tag{13}$$

is obtained, where $V(x,y,z,t)$ is the electrode potential at a given location and time. Substituting Eq. (13) into Eq. (12), it follows that:

$$\delta V(x,y,z,t) = 0. \tag{14}$$

On the other hand, an electrolytic current flows in the solution, caused by the mass transport of ionic species. Under the condition when large amount of supporting electrolyte is present, the z component of the current density vector is expressed [Eq. (5)] as

$$J_z(x,y,z,t) = -\sigma\left[\frac{\partial}{\partial z}V(x,y,z,t) - \frac{\partial}{\partial z}H(x,y,z,t) - \frac{\Phi(x,y,t)}{nF}\delta(z-Z)\right], \tag{15}$$

where σ is the electric conductivity, H the concentration overpotential for the active ion, Φ the surface potential arising from surface deformation, and $\delta(z-Z)$ is the δ function. The equation $z = Z$ depicts the electric double layer. In addition, $z = Z+0$ and $z = Z-0$ express the interfaces between the double layer and the solution and between the double layer and the metal surface, respectively. Integrating Eq. (15) from the bulk of the solution $z = \infty$ to a point on the interface $z = Z-0$, the equation

$$V(x,y,Z-0,t) - V(z=\infty) = \frac{1}{\sigma}\int_{Z-0}^{\infty} J_z(x,y,z,t)\, dz + H(x,y,Z+0,t) - H(z=\infty) - \frac{\Phi(x,y,t)}{nF} \tag{16}$$

is obtained. Here, $V(z=\infty)$ and $H(z=\infty)$ are the electrode potential and the concentration overpotential in the bulk of the solution, respectively. Considering $V(z=\infty)$ and

$H(z=\infty)$ constant, we take the variation of Eq. (16), then the following equation is obtained:

$$\delta V(x,y,Z-0,t)=\frac{1}{\sigma}\int_{Z-0}^{\infty} j_z(x,y,z,t)dz + \eta(x,y,Z+0,t)-\frac{\varphi(x,y,t)}{nF}, \tag{17}$$

where $j_z(x,y,z,t)$, $\eta(x,y,z,t)$, and $\varphi(x,y,t)$ are the fluctuation components of the z component of the electrolytic current density, the concentration overpotential, and the surface potential, respectively. Applying the condition represented by Eq. (14) to Eq. (17), the following equation is finally derived:

$$\frac{1}{\sigma}\int_{Z}^{\infty} j_z(x,y,z,t)\,dz+\eta(x,y,Z,t)-\frac{\varphi(x,y,t)}{nF}=0. \tag{18}$$

In view of Eq. (5) and the current density fluctuation, the explicit total current density at electrode surface is

$$J_z(x,y,Z,t)=-nFD\sqrt{\frac{1}{\pi Dt}} \times\{C^*(z=\infty)-C^*(z=Z^*)\}+j_z(x,y,Z,t),$$

where the first term on the right-hand side changes in the usual mode of $1/\sqrt{t}$ with time, and the second term, as will be discussed later, varies in exponential mode with time. During the early stage of deposition, it is reasonably assumed that the fluctuation term is much smaller than the nondisturbed first term. So, the current density measured follows the usual diffusion current equation [Eq. (5)]. This can be easily ascertained by experiments.

C. Concentration change near the electrode surface

As shown in the previous paper,[4] the nonperturbed term of the concentration of depositing ion in connection with the electrode surface is depicted as

$$C^*(Z,t)=C^*(Z^*,t)[\equiv C^*(z=Z^*)] \tag{19}$$

and the perturbed term as

$$c(x,y,Z,t)=c(x,y,Z^*,t)+L(t)\zeta(x,y,t), \tag{20}$$

where $\zeta(x,y,t)$ is the perturbed component of the surface height. $L(t)$ means the concentration gradient at the surface, i.e.,

$$L(t)=\left\{\frac{\partial C^*(z,t)}{\partial z}\right\}_{z=Z^*} =\sqrt{\frac{1}{\pi Dt}}\{C^*(z=\infty)-C^*(z=Z^*)\}, \tag{21}$$

where the last expression is derived from Eq. (5).

D. Mass balance of adatoms in the electric double layer

On reaching the electrode surface, the active ionic species receive some electrons from the electrode in the range of electric double layer to adsorb on the surface. Consequently, some of the adatoms diffuse to incorporate into the crystal lattice according to the potential difference on the surface, and others directly incorporate to form crystal nuclei. Figure 1 illustrates such a process schematically.

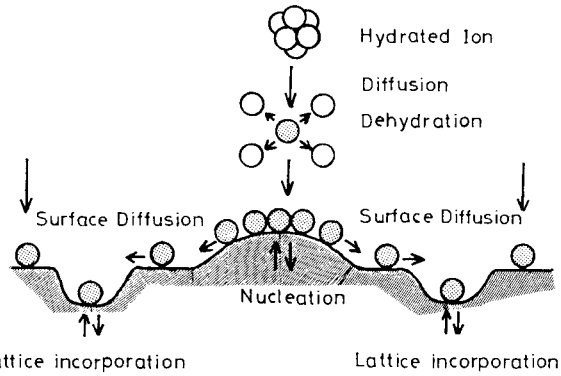

FIG. 1. Schematic profile of the mass balance in electrodeposition. On the electrode surface, both the surface diffusion of adatoms and the nucleation successively take place. Since electron-exchanging process is not rate determining, it is reasonably assumed that the adatoms remain in equilibrium with lattice atoms.

The mass balance of the adatoms in the double layer is described by the following:

$$\frac{\partial C_{ad}(x,y,t)}{\partial t}+\nabla_{\perp}\cdot\mathbf{J}_{surf} =J_{flux}(z=Z+0)-J_{flux}(z=Z-0), \tag{22}$$

where $z=Z+0$ and $z=Z-0$ denote the interfaces between the double layer and the bulk solution and between the double layer and the crystal lattice, respectively. $C_{ad}(x,y,t)$ is the concentration of the adatom, and $\nabla_{\perp}\equiv(\partial/\partial x,\partial/\partial y)$. $\mathbf{J}_{surf}$ is the mass flux density of the adatom

$$\mathbf{J}_{surf}=-D_{ad}\nabla_{\perp}C_{ad}(x,y,t)+bC_{ad}(x,y,t)\mathbf{f}. \tag{23}$$

The lateral flux density on the curved surface is, in general different from that on the flat surface parallel to the x–y plane. Using the lateral coordinates (X,Y), it follows that $\partial/\partial X=1/h_1\partial/\partial x$ and $\partial/\partial Y=1/h_2\partial/\partial y$, where $h_1=\{1+(\partial\zeta/\partial x)^2\}^{1/2}$ and $h_2=\{1+(\partial\zeta/\partial y)^2\}^{1/2}$. If the irregularity of the surface is not so high, $\partial/\partial X=\partial/\partial x$ and $\partial/\partial Y$ are derived. Hence, D_{ad} is the surface diffusion coefficient of adatoms, and b is the mobility which satisfied the Einstein relation

$$b=\frac{D_{ad}}{RT}. \tag{24}$$

$\mathbf{f}$ denotes a driving force arising from the potential difference caused by the surface deformation. Thus, it can be written as

$$\mathbf{f}=-\nabla_{\perp}\varphi(x,y,t). \tag{25}$$

On the other hand, J_{flux} $(z=Z+0)$ is the mass flux density flowing from the solution into the double layer. In view of the sign of the flux, the following equation is obtained:

$$J_{flux}(z=Z+0)=D\{\mathbf{n}\cdot\nabla C(x,y,z,t)\}_{z=Z+0}, \tag{26}$$

where $\mathbf{n}$ is the unit vector normal to the interface of the double layer. Eventually, $J_{flux}(z=Z-0)$ is the mass flux density of the adatoms entering or leaving the interface between the double layer and the crystal lattice, which occurs at the active sites of the lattice, e.g., kinks and steps.

Taking into consideration that the deposition determines the surface shape, the following relationship for the

morphological variation with deposition time is derived:

$$\frac{\partial Z(x,y,t)}{\partial t} = \Omega\left\{\frac{\partial C_{ad}(x,y,t)}{\partial t} + J_{flux}(z = Z - 0)\right\}. \quad (27)$$

Henceforth, substituting Eq. (27) into Eq. (22), the rate equation for the increase of surface height is written as follows:

$$\frac{1}{\Omega}\frac{\partial Z(x,y,t)}{\partial t} + \nabla_\perp \cdot \mathbf{J}_{surf} = J_{flux}(z = Z + 0), \quad (28)$$

where Ω is the molar volume of the crystal. In the present case, the deposition is not under reaction control but diffusion control, so that it can be reasonably assumed that a certain equilibrium relation exists between adatoms and lattice atoms, viz., the concentration of the adatoms is always equal to that at the equilibrium potential. (According to the measurements by Bockris *et al.*,[9,10] the equilibrium concentration of the adatoms at Ag electrode does not depend upon the bulk concentration of Ag ions and seems to keep constant. The existence of the equilibrium between adatoms and lattice atoms leads to the absence of the macroscopic gradient of adatom concentration as far as the activity of lattice atoms is assumed constant along with a surface.) With Eqs. (23)–(28), the equation for the surface fluctuation is finally obtained:

$$\frac{1}{\Omega}\frac{\partial\zeta(x,y,t)}{\partial t} = \frac{D_{ad}}{RT} C^*_{ad} \nabla_\perp^2 \varphi(x,y,t) + D\left\{\frac{\partial c(x,y,z,t)}{\partial z}\right\}_{z=Z^*}. \quad (29)$$

E. Other fundamental relationships

Concentration overpotential, in the presence of large amount of supporting electrolyte, can be written in the form

$$H(x,y,z,t) = \frac{RT}{nF}\ln\left\{\frac{C(x,y,z,t)}{C^*(z=\infty)}\right\}. \quad (30)$$

Taking the variation of Eq. (30) in view that $C^*(z=\infty)$ is constant, it follows that $\delta H(x,y,z,t) = (RT/nF)\cdot\delta C(x,y,z,t)/C(x,y,z,t)$. Here, $\eta(x,y,z,t) = \delta H(x,y,z,t)$, $c(x,y,z,t) = \delta C(x,y,z,t)$, and $C(x,y,z,t) = C^*(z,t) + c(x,y,z,t)$. Consequently, neglecting higher order of smallness, the equation

$$\eta(x,y,z,t) = \frac{RT}{nF}\frac{c(x,y,z,t)}{C^*(z,t)} \quad (31)$$

is derived. The fluctuation component of an electrolytic current possesses the well-known relationship with the mass flux of the depositing ion at the interface, as follows:

$$j_z(x,y,Z,t) = -nFD\left\{\frac{\partial}{\partial_z} c(x,y,z,t)\right\}_{z=Z}. \quad (32)$$

The equation for the increment of the surface potential arising from surface deformation is obtained from the Laplace equation for small deformation[12]

$$\varphi(x,y,t) = -\Omega\gamma\nabla_\perp^2\zeta(x,y,t), \quad (33)$$

where γ is the surface energy of the electrode.

F. Derivation of the dsi equation

The fluctuation component of current density in a solution is derived from Eqs. (14) and (15), as follows:

$$\mathbf{j}(x,y,z,t) = \sigma\nabla\eta(x,y,z,t). \quad (34)$$

Since the current density is conserved in the solution, the following conservation equation of current fluctuation is obtained:

$$\nabla\cdot\mathbf{j} = 0. \quad (35)$$

Substituting Eq. (34) into Eq. (35), it follows that:

$$\nabla^2\eta(x,y,z,t) = 0. \quad (36)$$

Then, performing Fourier transformation of the left-hand side of Eq. (36) concerning x and y, the image function, $\eta^0(z,t)$ of $\eta(x,y,z,t)$ gives the following equation:

$$\left(\frac{\partial^2}{\partial z^2} - k^2\right)\eta^0(z,t) = 0. \quad (37)$$

Adopting a boundary condition, $\eta^0(z,t)\to 0$ as $z\to\infty$, the solution of Eq. (37) is obtained as

$$\eta^0(z,t) = B_1 e^{-kz}\beta(t), \quad (38)$$

where $\beta(t)$ is an arbitrary function of t, and B_1 is an arbitrary constant.

From Eq. (34), the z component of $\mathbf{j}(x,y,z,t)$ has the following relationship with $\eta(x,y,z,t)$:

$$j_z(x,y,z,t) = \sigma\frac{\partial}{\partial z}\eta(x,y,z,t). \quad (39)$$

By carrying out Fourier transformation of both sides of Eq. (39) with regard to x and y, the equation of the image functions $j_z^0(z,t)$ and $\eta^0(z,t)$ for $j_z(x,y,z,t)$ and $\eta(x,y,z,t)$ is given in the form

$$j_z^0(z,t) = \sigma\frac{\partial}{\partial z}\eta^0(z,t). \quad (40)$$

Substitution of Eq. (38) into Eq. (40) leads to the equation

$$j_z^0(z,t) = -\sigma B_1 k e^{-kz}\beta(t). \quad (41)$$

Then, performing Fourier transformation of the both sides of Eq. (32) concerning x and y, the equation

$$j_z^0(z,t) = -nFD\frac{\partial}{\partial z}c^0(z,t) \quad \text{for } z = Z \quad (42)$$

is obtained. From Eqs. (11), (41), and (42), the following equation for the interface $z = Z$ is derived:

$$j_z^0(Z,t) = nFDkc^0(Z^*,t), \quad (43)$$

where the relation $\exp(-kZ) = \exp(-kZ^*)$ is used, which holds within the first approximation as far as $\zeta(x,y,t)$ is small.

Substitution of Eq. (20) into Eq. (31) allows the expression at $z = Z$,

$$\eta(x,y,Z,t) = \frac{RT}{nF}\frac{c(x,y,Z^*,t) + L(t)\zeta(x,y,t)}{C^*(z=Z^*)}, \quad (44)$$

where Eq. (19), $C^*(Z,t) = C^*(z=Z^*)$ is used. Applying Fourier transformation to Eq. (44) with respect to x and y, the equation

$$\eta^0(Z,t) = \frac{RT}{nF}\frac{c^0(Z^*,t) + L(t)\zeta^0(t)}{C^*(z=Z^*)} \quad (45)$$

is derived, where $\zeta^0(t)$ is the image function of $\zeta(x,y,t)$. The following equation is then obtained by the Fourier transformation for Eq. (33):

$$\varphi^0(t) = \Omega\gamma k^2 \zeta^0(t). \tag{46}$$

For Eq. (18), the Fourier transformation concerning x and y yields

$$\frac{1}{\sigma}\int_Z^\infty j_z^0(z,t)dz + \eta^0(Z,t) - \frac{\varphi^0(t)}{nF} = 0. \tag{47}$$

Hence, from Eqs. (41) and (43), the equation

$$\int_Z^\infty j_z^0(z,t)dz = nFDc^0(Z^*,t) \tag{48}$$

is derived. Substitution of Eqs. (45), (46), and (48) into Eq. (47) gives the relationship between $c^0(Z^*,t)$ and $\zeta^0(t)$ as follows:

$$c^0(Z^*,t) = \frac{\sigma\{\Omega\gamma C^*(z=Z^*)k^2 - RTL(t)\}\zeta^0(t)}{(nF)^2 DC^*(z=Z^*) + \sigma RT}. \tag{49}$$

Finally, Eq. (29) is transformed by the Fourier image functions with regard to x and y in the form

$$\frac{1}{\Omega}\frac{d\zeta^0(t)}{dt} = -\frac{D_{ad}}{RT}C_{ad}^* k^2 \varphi^0(t) + D\left\{\frac{\partial c^0(z,t)}{\partial z}\right\}_{z=Z^*}. \tag{50}$$

Using Eqs. (42) and (43), the equation of $c^0(Z^*,t)$ is given as

$$\left\{\frac{\partial c^0(z,t)}{\partial z}\right\}_{z=Z^*} = -kc^0(Z^*,t). \tag{51}$$

From Eqs. (46), (49)–(51):

$$\frac{d\zeta^0(t)}{dt} = f(k,t)\zeta^0(t), \tag{52}$$

where

$$f(k,t) = \frac{\sigma\Omega Dk\{RTL(t) - \Omega\gamma C^*(z=Z^*)k^2\}}{(nF)^2 DC^*(z=Z^*) + \sigma RT} - \frac{D_{ad}C_{ad}^*\Omega^2\gamma k^4}{RT}. \tag{53}$$

The product $RTL(t)$ in the numerator of the first fraction depicts the unstable growth term owing to the positive concentration gradient in the case of deposition, on the other hand, $\Omega\gamma C^*(z=Z^*)k^2$ provides a stabilization effect accompanied with the change of surface potential caused by surface deformation. The second fraction makes the nucleation growth to suppress by the surface diffusion of adatoms.

In terms of the image function $\zeta^0(0)$ of the initial surface fluctuation, the solution of Eq. (52) is given by

$$\zeta^0(t) = \zeta^0(0)\exp\left\{\int_0^t f(k,t)dt\right\}. \tag{54}$$

This introduces an exponential mode of time to the growth of surface irregularity. Therefore, the surface fluctuation having a single set of arbitrary wave numbers (k_x, k_y) is expressed as

$$\zeta_k(x,y,t) = \zeta^0(t)\exp[i(k_x x + k_y y)]. \tag{55}$$

$\zeta^0(t)$ means the peak height of a sinusoidally formed surface, exhibited in Fig. 3. Henceforth, the degree of surface irregularity (dsi) is introduced by

$$\ln\{\zeta_k(x,y,t)/\zeta_k(x,y,0)\} = \int_0^t f(k,t)dt. \tag{56}$$

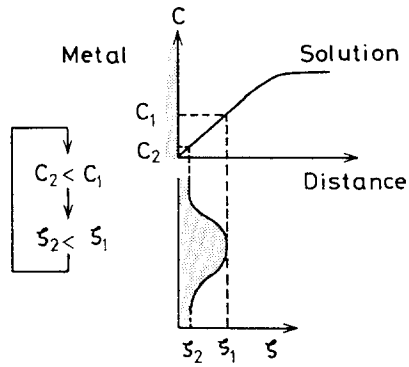

FIG. 2. The process of occurrence of the morphological instability. In electrodeposition, since the concentration gradient of metal ion is formed in positive value, the convex portion ζ_1 of the surface irregularity tends to project into higher concentration region than the concave place ζ_2. The surface concentration C_1 of the depositing ion at ζ_1 becomes higher than the concentration C_2 at ζ_2, so that the mass flux at ζ_1 increases more rapidly than at ζ_2; the higher the part the more it protrudes, and this process proceeds in the form of a kind of positive feedback cycle.

Namely, dsi becomes a measure of the vertical growth rate of crystal peak, and in addition, the wavelength λ which has a relationship with wave number k in the form of $\lambda \equiv 2\pi/k$ is used as a measure of the lateral size of the peak.

Comparing Eq. (53) with the result of the preceding paper, it is found that the new term $-D_{ad}C_{ad}^*\Omega^2\gamma k^4/RT$ adds

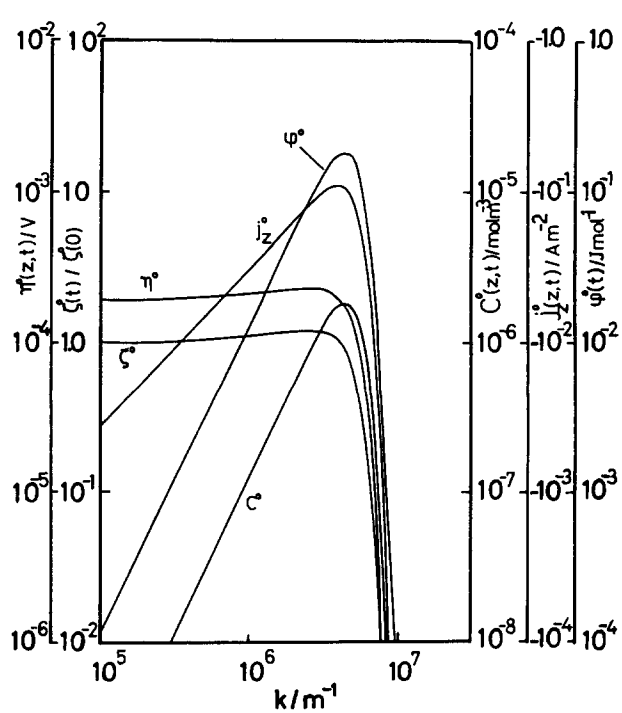

FIG. 3. Plots of the various fluctuations vs wave number at the peaks of sinusoidally formed surface after 5 s of deposition time.
$\eta^0(Z,t)$, $\zeta^0(t)$, $c^0(Z,t)$, $j_z^0(Z,t)$, and $\varphi^0(t)$ are the Fourier image functions of $\eta(x,y,Z,t)$, $\zeta(x,y,t)$, $c(x,y,Z,t)$, $j_z(x,y,Z,t)$, and $\varphi(x,y,t)$, respectively. Applied potential is -0.3 V, and the concentration of the electrolyte solution is 56.8 mol m^{-3}. $D = 1.55\times10^{-9}$ m^2 s^{-1}, $\sigma = 1.7\times10^2$ Ω^{-1} m^{-1}, $\Omega = 1.03\times10^{-5}$ m^3 mol^{-1}, $\gamma = 1.1$ J m^{-2}, $D_{ad} = 2.2\times10^{-10}$ m^2 s^{-1}, $C_{ad}^* = 8.0\times10^{-6}$ mol m^{-2}, and $T = 300$ K. These are based on the experimental data for silver deposition.

to the right-hand side of $f(k,t)$, which describes the contribution of the surface diffusion of adatoms; this always takes negative value. Thus it is concluded that the surface diffusion tends to suppress the development of surface irregularity. At the same time, because the surface diffusion term has the fourth order of wave number, for markedly small crystal particles which have quite large wave number, surface diffusion may give the most striking effect. Substituting Eq. (21) into Eq. (53), and then integrating $f(k,t)$ in accordance with Eq. (56), the dsi equation is explicitly written as

$$\ln\{\zeta_k(x,y,t)/\zeta_k(x,y,0)\} = \frac{\sigma\Omega D\left[2RT\sqrt{t/\pi D}\{C^*(z=\infty)-C^*(z=Z^*)\}-\Omega\gamma C^*(z=Z^*)tk^2\right]k}{(nF)^2DC^*(z=Z^*)+\sigma RT} - \frac{D_{ad}C^*_{ad}\Omega^2\gamma t}{RT}k^4. \quad (57)$$

Here, this is derived from the component of surface fluctuation for a single wave number k and its initial value. Thus, it can be said that the dsi equation expresses how to grow the surface fluctuation with a given wavelength. In this dsi equation, the term of $\sqrt{t}$ appears instead of $1/\sqrt{t}$ which is characteristic of ordinal diffusion current. This can be attributed to the integration of the concentration gradient $L(t)(\propto 1/\sqrt{t})$ in Eq. (53) according to Eq. (56).

From Eq. (30), the surface concentration, $C^*(z=Z^*)$ in the nondisturbed state is determined by

$$C^*(z=Z^*) = C^*(z=\infty)\exp\left\{\frac{nF}{RT}H^*(z=Z^*)\right\}. \quad (58)$$

The concentration overpotential $H^*(z=Z^*)$ at the nondisturbed surface is defined negative for cathodic polarization.

III. RESULTS AND DISCUSSION

A. Occurrence of instability

From Eq. (57), it is found that dsi has positive values for a certain range of wave number in cathodic deposition, but not for all the range of wave numbers in anodic dissolution. This means that only in the case of cathodic deposition, the electrode system becomes unstable, i.e., unstable crystal growth occurs. Such unstable deposition can be thought to take place according to the following process; as illustrated schematically in Fig. 2, active ionic species in the deposition forms such a concentration distribution that the concentration increases with the increasing distance from the electrode surface. Hence, the convex parts of surface irregularity protrude into higher concentration area of the solution than the concave parts. The mass flux at the top portion, thus becomes larger than at the bottom, so that the top still more extends into the bulk of the solution.

In addition, the mechanism of such growth is also reinforced by the thermodynamic condition [Eq. (18)] for the mass transfer in the solution. Namely, at the peak of the irregularity, the increment of surface potential is positive, and at the same place, the current density is higher than the average value. Since the nondisturbed current density is defined negative for cathodic polarization, the fluctuation component, $j_z(x,y,z,t)$ at the peak becomes negative. In view of the direction of the integration,

$$\int_z^\infty j_z(x,y,z,t)dz < 0 \quad (59)$$

holds at the peak point. Then, from Eq. (18), the variation of the concentration overpotential $\eta(x,y,z,t)$ at the surface $z=Z$ is

$$\eta(x,y,z,t) = -\frac{1}{\sigma}\int_z^\infty j_z(x,y,z,t)dz + \frac{\varphi(x,y,t)}{nF}. \quad (60)$$

$\eta(x,y,Z,t)$ increases in the positive direction with increasing time as far as $j_z(x,y,z,t)$ and $\varphi(x,y,t)$ increase in the negative and positive directions, respectively. The behaviors of such quantities at the interface $\eta(x,y,Z,t)$, $\zeta(x,y,t)$, $c(x,y,Z,t)$, $j_z(x,y,Z,t)$, and $\varphi(x,y,t)$ may be understood by inspecting their image functions $\eta^0(Z,t)$, $\zeta^0(t)$, $c^0(Z,t)$, $j_z^0(Z,t)$, and $\varphi^0(t)$, which depict the values of the fluctuations at the peaks of a sinusoidally formed surface with a single wave number. As shown in Fig. 3, the absolute values of the all components abruptly decrease nearly at the same region of wave number. However, there are two types of the function forms, $\eta^0(Z,t)$ and $\zeta^0(Z,t)$ have plateaus while $c^0(Z,t)$, $j_z^0(Z,t)$, and $\varphi^0(t)$ exhibit maxima. And as expected above, the sign of $j_z(x,y,Z,t)$ at the peaks $[j_z^0(Z,t)]$ is surely negative. The positive increase of $\eta(x,y,Z,t)$ with time indicates that at projecting portion, the concentration overpotential decreases because its nondisturbed value is defined negative for the deposition. As a

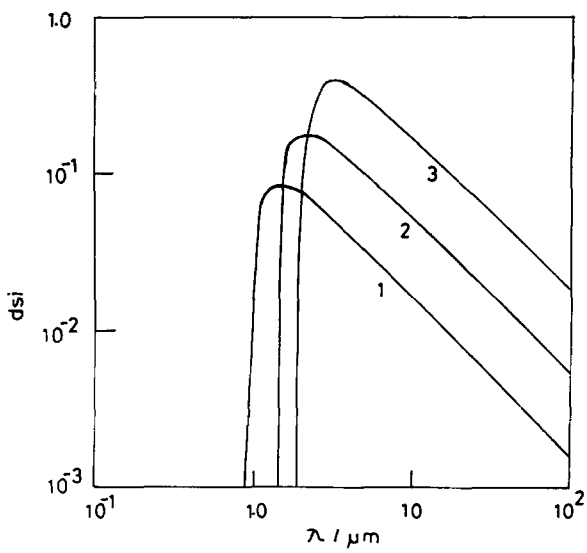

FIG. 4. Variation in the degree of surface irregularity (dsi) with wavelength at various deposition times after a constant potential step of -0.3 V is imposed. The concentration of silver ionic solution is 56.8 mol m^{-3}. Curve 1: 1.0 s, curve 2: 10.0 s, and curve 3: 100.0 s. Other data for calculation are the same as Fig. 3.

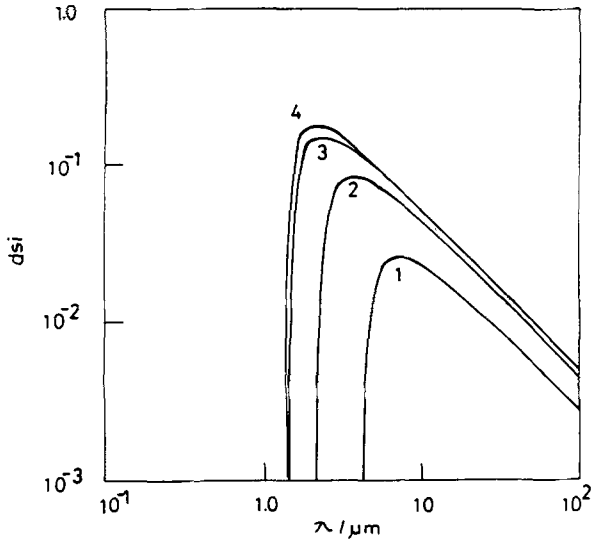

FIG. 5. Variation in the degree of surface irregularity (dsi) with wavelength at the deposition time of 10.0 s after a constant potential step of − 0.3 V is applied. The concentration of silver ionic solution is 56.8 mol m^{-3}. Curve 1: − 0.02 V, curve 2: − 0.05 V, curve 3: − 0.1 V and curve 4: − 0.2 V. Other data for calculation are the same as Fig. 3.

result, it is concluded that the projection of the peak is also accelerated by the decrease of the concentration overpotential.

B. Effect of the surface diffusion of adatoms

Figures 4 and 5 display several typical dsi–λ curves. Here, λ is the wavelength of a sinusoidal surface irregularity.

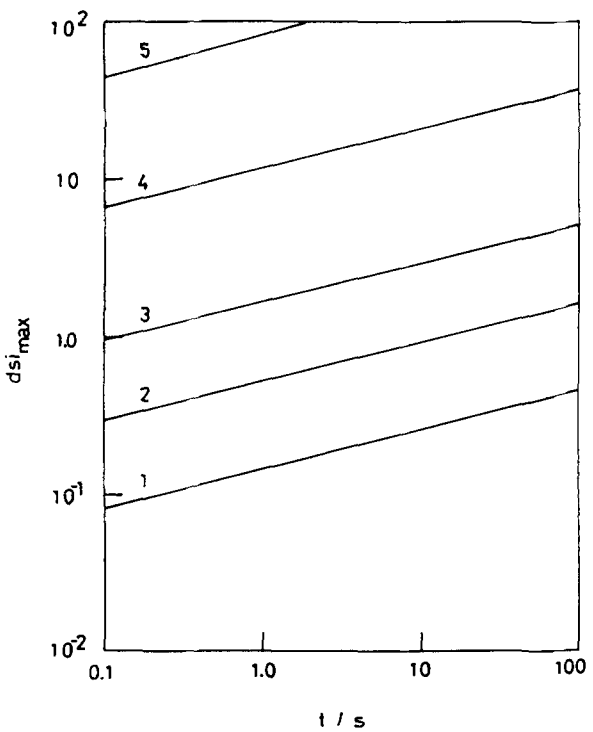

FIG. 6. Behavior of the maximum degree of surface irregularity dsi_{max} as a function of deposition time for various applied overpotential in the case neglecting surface diffusion effect. Curve 1: − 0.02 V, curve 2: − 0.05 V, curve 3: − 0.1 V, curve 4: − 0.2 V, and curve 5: − 0.3 V. Other data except for $D_{ad} = 0$ are the same as Fig. 3.

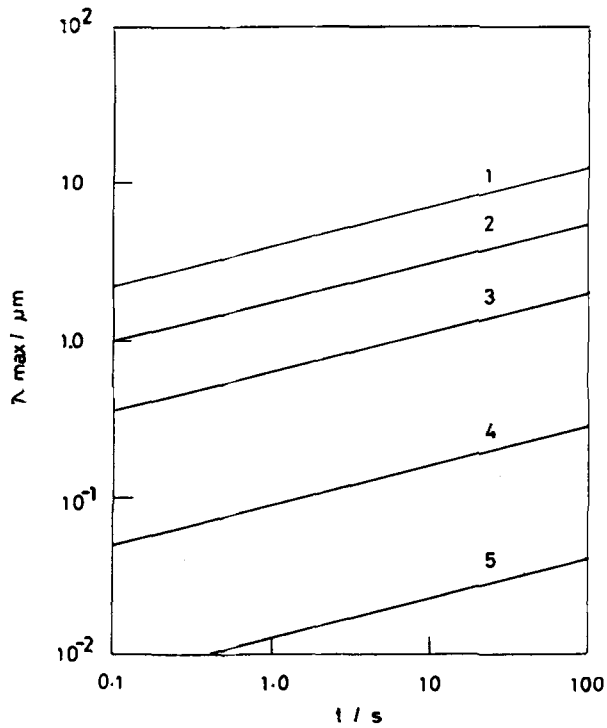

FIG. 7. Behavior of the wavelength, λ_{max} corresponding to dsi_{max} in Fig. 6 as a function of deposition time for various applied overpotential in the case neglecting surface diffusion effect. Curve 1: − 0.02 V, curve 2: − 0.05 V, curve 3: − 0.1 V, curve 4: − 0.2 V, and curve 5: − 0.3 V. Other data except for $D_{ad} = 0$ are the same as Fig. 3.

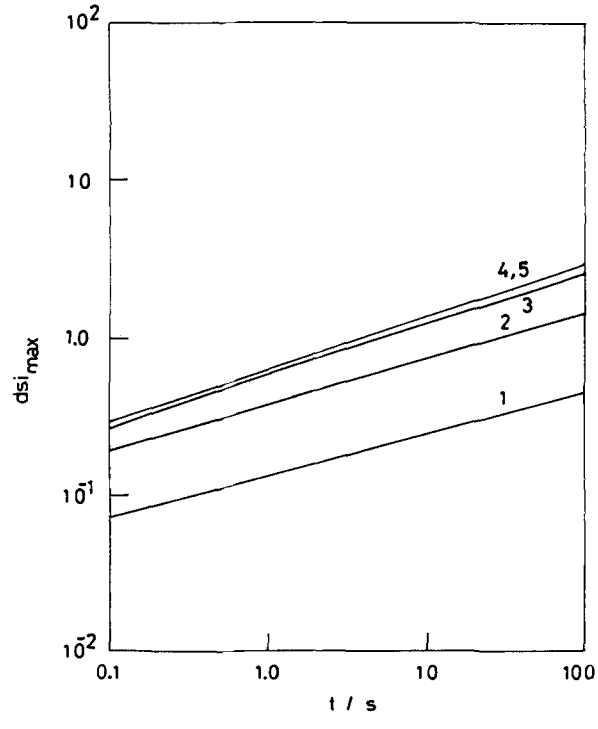

FIG. 8. dsi_{max}-deposition time curves for some applied overpotentials in view of surface diffusion of adatoms: $D_{ad} = 5.0\times10^{-10}$ m^2 s^{-1}, and $C^*_{ad} = 8.0\times10^{-6}$ mol m^{-2}. Curve 1: − 0.02 V, curve 2: − 0.05 V, curve 3: − 0.1 V, curve 4: − 0.2 V, and curve 5: − 0.3 V. Other data are the same as Fig. 3.

The data of the parameters used for calculation are those for silver deposition onto a silver electrode, and the values of surface diffusion constant and adatom concentration are determined in consideration of the data by Bockris *et al.*[9,10,13] Every curve illustrated has one maximum value for a certain wavelength.

Furthermore, in order to make clear the whole analytical behavior of dsi, at first the following equation neglecting the surface diffusion was obtained:

$$\ln\{\zeta_k(x,y,t)/\zeta_k(x,y,0)\} = \frac{\sigma\Omega D\,[2RT\sqrt{t/\pi D}\,\{C^*(z=\infty)-C^*(z=Z^*)\}-\Omega\gamma C^*(z=Z^*)tk^2]k}{(nF)^2DC^*(z=Z^*)+\sigma RT}. \tag{61}$$

The maximum dsi is easy to write in the following way:

$$\mathrm{dsi}_{\max} = \frac{4\sqrt{6}}{9} \times \frac{\sigma D^{1/4}\Omega^{1/2}[RT\{C^*(z=\infty)-C^*(z=Z^*)\}]^{3/2}t^{1/4}}{\pi^{3/4}\{\gamma C^*(z=Z^*)\}^{1/2}\{D(nF)^2C^*(z=Z^*)+\sigma RT\}}. \tag{62}$$

Consequently, the wavelength corresponding to $\mathrm{dsi}_{\max}$ is given as

$$\lambda_{\max} = 2\pi\sqrt{\frac{3\Omega\gamma C^*(z=Z^*)\sqrt{\pi Dt}}{2RT\{C^*(z=\infty)-C^*(z=Z^*)\}}}. \tag{63}$$

Obviously, $\mathrm{dsi}_{\max}$ increases with increasing concentration overpotential, in this case where the surface diffusion is ignored, finally diverging into infinity. If the $\mathrm{dsi}_{\max}$ is taken as a measure of the growth rate, this means that the crystal growth is markedly promoted by the increase of the overpotential. On the other hand, $\lambda_{\max}$ decreases with concentration overpotential, in the present case, finally converging to zero. Taking $\lambda_{\max}$ as a measure of crystal size, it becomes infinitesimal at maximum cathodic potentials.

The plots of the $\mathrm{dsi}_{\max}$ and $\lambda_{\max}$ vs deposition time in the case where the surface diffusion is neglected are represented in Figs. 6 and 7, respectively. The figures show how the $\mathrm{dsi}_{\max}$ and $\lambda_{\max}$ increase with increasing time. The slopes of the $\mathrm{dsi}_{\max}$-time and $\lambda_{\max}$-time curves are consistent with 1/4, as predicted by Eqs. (62) and (63). Figure 6 indicates that the $\mathrm{dsi}_{\max}$ increases as much as one order of magnitude per 100 mV, while for $\lambda_{\max}$, Fig. 7 shows that it decreases as much as one order of magnitude per 100 mV. Therefore, when $H^*(z=Z^*)$ increases in the cathodic direction, an unrealistic prediction emerges, i.e., at high cathodic polarization, a lot of infinitesimal crystal particles are yielded at extremely high growth rate. Such a result would be reasonably understood in view of the high supersaturation of the adatoms on the electrode in the limiting current region. At such high cathodic overpotential, the surface concentration of the ions approaches zero as the electrode potential shifts to the higher cathode region; finally supersaturation allows the

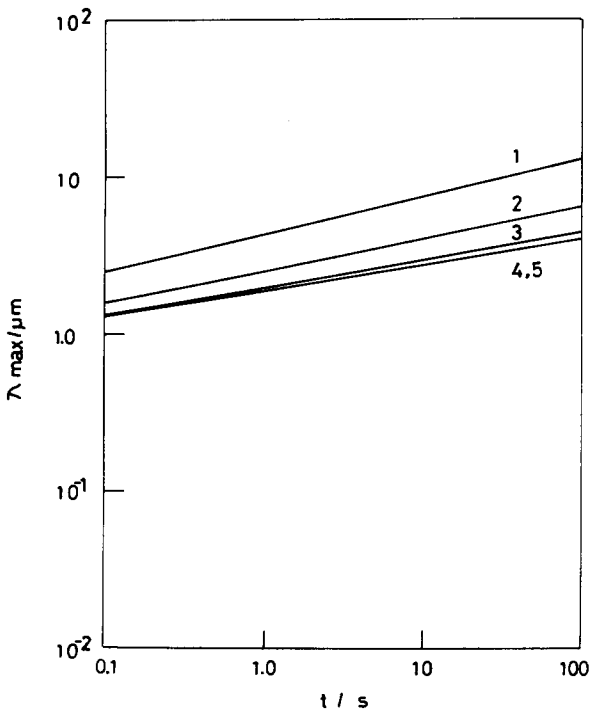

FIG. 9. $\lambda_{\max}$—deposition time curves for some applied overpotentials in view of surface diffusion of adatoms. Curve 1: − 0.02 V, curve 2: − 0.05 V, curve 3: − 0.1 V, curve 4: − 0.2 V, and curve 5: − 0.3 V. Other data are the same as Fig. 8.

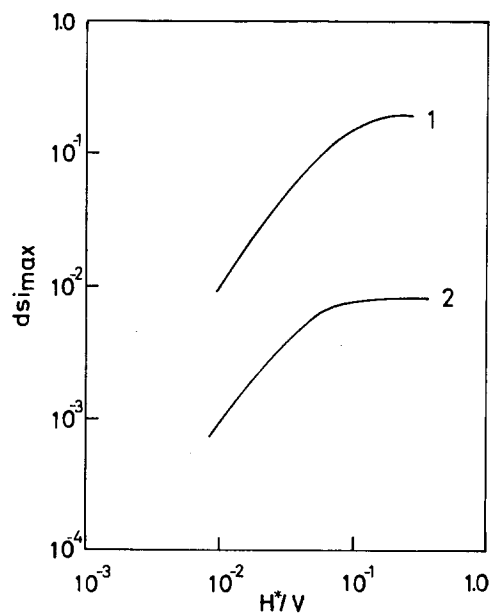

FIG. 10. Relationship between the maximum degree of surface irregularity $\mathrm{dsi}_{\max}$ and applied overpotential $H^*(z=Z^*)$ at the deposition time of 10.0 s. Curve 1: 56.8 mol m^{-3}, and curve 2: 5.68 mol m^{-3}. Other data are the same as Fig. 8.

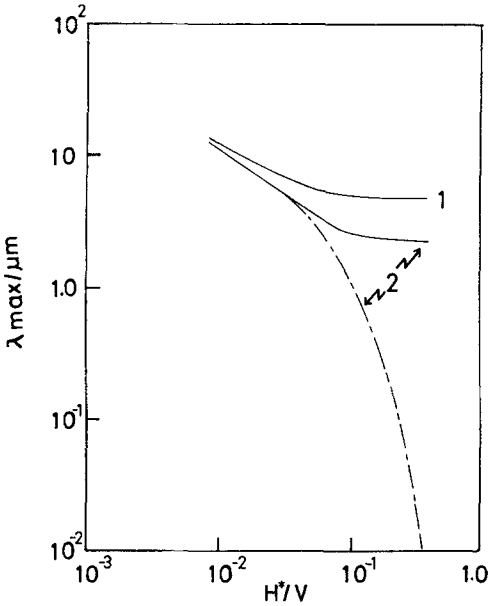

FIG. 11. Relationship between the wavelength λ_{max} corresponding to dsi_{max} in Fig. 10 and applied concentration overpotential $H^*(z = Z^*)$ at the deposition time of 10.0 s. ——: $D_{ad} = 2.2\times10^{-10}$ m^2 s^{-1}, — — —: $D_{ad} = 0.0$ m^2 s^{-1}. Curve 1: 5.68 mol m^{-3}, and curve 256.8 mol m^{-3}. Other data are the same as Fig. 8.

electrode surface to generate numerous small crystals continuously through multiple nucleation.

The surface diffusion of adatoms is, on the contrary, moderates such a situation, i.e., there is release of adatoms from concentrated nucleation sites to active lattice points, such as kinks and steps. In practice, choosing several overpotentials for the deposition, dsi_{max}-time and λ_{max}-time curves including the surface diffusion were calculated as shown in Figs. 8 and 9, respectively. The dsi_{max}-time curves have the slope of 1/4 at the lower potentials while the slopes at the higher potentials approach 1/3. The λ_{max}-time curves also have the slope of 1/4 at the lower potentials, and the slopes decrease toward 1/6 with increasing potential. These results indicate that there is no influence on surface diffusion at low polarization, but at high potentials, the crystal growth mode is affected by such the diffusion.

For better comprehension, the dependence of the dsi_{max} and λ_{max} on the concentration overpotential is represented in Figs. 10 and 11. It is obviously found in the figures that the λ_{max} increases and the increasing rate of the dsi_{max} diminishes until they attain certain values owing to the same effect of the surface diffusion. We can easily expect that the crystals formed grow in the tangential direction, and the growth in the direction vertical to the surface becomes slower with increasing overpotential. It can also be seen that in the region of the diffusion-limiting current, the behaviors of the dsi_{max} and λ_{max} do not depend on applied overpotential, which leads to a prediction that the crystal formation may be indifferent to high overpotential. The prediction was supported by SEM observations. Here, one should note the fact that all the calculations in this paper were carried out using the same value of surface energy. Therefore, it can also be concluded that the surface energy should become constant in the limiting current region.

IV. CONCLUSION

In order to solve some severe difficulties, viz, the divergence of dsi_{max} to infinity and the corresponding convergence of λ_{max} to infinitesimal values in the limiting current region, the dsi equation for nonsteady potentiostatic deposition was examined in view of the effect of surface diffusion of adatoms.

Consequently, it was found that the difficulties disappear because the surface diffusion provides a large compensating effect in relation to dsi_{max} and λ_{max}, particularly at high cathodic potentials. At the same time, it was also predicted that the size and growth rate of the crystals formed are independent of the overpotential in such region.

ACKNOWLEDGMENT

Publication costs of this article were assisted by the Institute of Vocational Training.

APPENDIX: NOMENCLATURE

t:	deposition time (s).
x,y,z:	variables in Cartesian coordinate system (m).
Z:	electrode surface height (m).
Z^*:	nonperturbed component of Z (m).
$Z+0$:	the height of the interface between the double layer and the solution (m).
$Z-0$:	the height of the interface between the double layer and the crystal lattice (m).
$\zeta(x,y,t)$:	fluctuation component of the surface height (m).
$\zeta_k(x,y,t)$:	equation of $\zeta(x,y,t)$ having a single set of wave numbers (k_x,k_y), (m).
$\zeta^0(t)$:	Fourier image function of $\zeta(x,y,t)$.
$C(x,y,z,t)$:	concentration of depositing ion (mol m^{-3}).
$C^*(z,t)$:	nonperturbed component of $C(x,y,z,t)$ (mol m^{-3}).
$C^*(z=\infty)$:	bulk concentration of depositing ion (mol m^{-3}).
$C^*(z=Z)$:	nonperturbed component of $C(x,y,z,t)$ at $z=Z$ (mol m^{-3}).
$C^*(z=Z^*)$:	nonperturbed component of $C(x,y,z,t)$ at $z=Z^*$ (mol m^{-3}).
$c(x,y,z,t)$:	fluctuation component of $C(x,y,z,t)$ (mol m^{-3}).
$c^0(z,t)$:	Fourier image function of $c(x,y,z,t)$.
$C_{ad}(x,y,t)$:	adatom concentration (mol m^{-2}).
C^*_{ad}:	equilibrium adatom concentration (mol m^{-2}).
$\mathbf{J}(x,y,z,t)$:	Current density (A m^{-2}).
$J^*_z(t)$:	Nonperturbed z component of $\mathbf{J}(x,y,z,t)$ (A m^{-2}).
$\mathbf{j}(x,y,z,t)$:	Fluctuation component of $\mathbf{J}(x,y,z,t)$ (A m^{-2}).
$j_z(x,y,z,t)$:	z component of $\mathbf{j}(x,y,z,t)$ (A m^{-2}).
$j^0_z(z,t)$:	Fourier image function of $j_z(x,y,z,t)$.
$\mathbf{J}_{surf}$:	Mass flux of adatom (mol s^{-1}m^{-1}).
$J_{flux}(z=Z+0)$:	Mass flux of depositing ion entering vertically to the double layer (mol s^{-1} m^{-2}).

$J_{flux}(z = Z - 0)$: Mass flux of adatom coming in and out the interface between the double layer and the metal surface (mol s^{-1} m^{-2}).
$V(x, y,z,t)$: Electrode potential (V).
$V(z = \infty)$: $V(x, y,z,t)$ at the bulk solution (V).
$V(x, y,z,t)$: Variation of $V(x, y,z,t)$, (V).
$H(x, y,z,t)$: Concentration overpotential of depositing ion (V).
$H(z = \infty)$: $H(x, y,z,t)$ at the bulk solution (V).
$H^*(z = Z^*)$: Nonperturbed component of $H(x, y,z,t)$ at $z = Z^*$, (V).
$\eta(x, y,z,t)$: Fluctuation component of $H(x, y,z,t)$ (V).
$\eta^0(z,t)$: Fourier image function of $\eta(x, y,z,t)$.
D: Diffusion coefficient of depositing ion (m^2 s^{-1}).
D_{ad}: Surface diffusion coefficient of adatom (m^2 s^{-1}).
F: Faraday constant (96 500 Coulomb equivalent^{-1}).
R: Gas constant (8.31 J deg^{-1} mol^{-1}).
T: Absolute temperature (K).
$L(t)$: Concentration gradient of depositing ion at the electrode surface (mol m^{-4}).
A_1: Arbitrary constant (mol m^{-3}).
A_2: Arbitrary constant (mol m^{-3}).
B_1: Arbitrary constant (mol m^{-3}).
b: Mobility of adatom (mol m^2 J^{-1} s^{-1}).
dsi: Degree of surface irregularity.
dsi_{max}: Maximum value of dsi.
f: Motive force of surface diffusion (N mol^{-1}).
$f(k,t)$: Function defined by Eq. (55).
i: $\equiv\sqrt{-1}$.
k: Wave number $(k_x^2 + k_y^2)^{1/2}$.
k_x, k_y: x and y components of wave number (m^{-1}).
n: Electron number exchanging at the electrode per one depositing ion.
n: Unit vector normal to the electrode surface.
$\Phi(x, y,t)$: Surface potential arising from surface deformation (J mol^{-1}).
$\varphi(x, y,t)$: Perturbed component of Φ (J mol^{-1}).
$\varphi^0(t)$: Fourier image function of $\varphi(x, y,t)$.
$\Psi(x, y,z,t)$: Electrochemical potential of depositing ion (V).
$\delta\Psi(x, y,z,t)$: Variation of $\Psi(x, y,z,t)$ (V).
$\alpha(t)$: Arbitrary function of deposition time.
$\beta(t)$: Arbitrary function of deposition time.
λ: Wavelength (m).
λ_{max}: Wavelength corresponding to dis_{max} (m).
$\delta(z - Z)$: δ function.
γ: Surface energy (J m^{-2}).
Ω: Molar volume of metal (m^3 mol^{-1}).
σ: Electric conductivity (Ω^{-1} m^{-1}).
∇: $\equiv(\partial/\partial x, \partial/\partial y, \partial/\partial z)$.
$\nabla_\perp$: $\equiv(\partial/\partial x, \partial/\partial y)$.

[1] N. Ibl, in *Advances in Electrochemistry and Electrochemical Engineering*, edited by P. Delahay and C. W. Tobias (Wiley, New York, 1962), Vol. 2, p. 49.
[2] N. Ibl, Helv. Chim. Acta **37**, 1149 (1954).
[3] I. Atanasiu and A. Calusaru, Stud. Cercet. Metal. **2**, 337 (1957); Chem. Abs. **52**, 1340h (1958).
[4] R. Aogaki, K. Kitazawa, Y. Kose, and K. Fueki, Electrochim. Acta **25**, 965 (1980).
[5] R. Aogaki and T. Makino, Electrochim. Acta **26**, 1509 (1981).
[6] R. Aogaki, J. Electrochem. Soc. **129**, 2442 (1982).
[7] R. Aogaki, J. Electrochem. Soc. **129**, 2447 (1982).
[8] T. Makino and R. Aogaki, Denki Kagaku **51**, 289 (1983).
[9] W. Mehl and J. O'M. Bockris, J. Chem. Phys. **27**, 817 (1957).
[10] W. Mehl and J. O'M. Bockris, Can. J. Chem. **37**, 190 (1959).
[11] P. Glansdorff and I. Prigogine, in *Thermodynamic Theory of Structure, Stability and Fluctuations* (Wiley–Interscience, London, 1971), Chap. 2, Sec. 2.
[12] L. D. Landau and E. M. Lifshitz, in *Fluid Mechanics* (Pergamon, Oxford, 1960), Chap. 7.
[13] J. O'M. Bockris and G. A. Razumney, in *Fundamental Aspects of Electrocrystallization* (Plenum, New York, 1967), p. 64.
[14] R. Aogaki and T. Makino, J. Electrochem. Soc. **131**, 40 (1984).
[15] R. Aogaki and T. Makino, J. Electrochem. Soc. **131**, 47 (1984).